Journal of Applied Polymer Science

Biomineralized Polypropylene/$CaCO_3$ Composite Nonwoven Meshes for Oil/Water Separation

Ke Liao, Xiang-Yu Ye, Peng-Cheng Chen, Zhi-Kang Xu

MOE Key Laboratory of Macromolecular Synthesis and Functionalization, Department of Polymer Science and Engineering, Zhejiang University, Hangzhou 310027, People's Republic of China

Correspondence to: Z.-K. Xu (E-mail: xuzk@zju.edu.cn)

ABSTRACT: Polypropylene/calcium carbonate ($CaCO_3$) composite nonwoven meshes were prepared on the basic principle of biomineralization by using a facile alternate soaking process (ASP) within 20 min. Negatively charged poly(acrylic acid) brushes, which can induce $CaCO_3$ nucleation, were first tethered onto the fiber surface of polypropylene nonwoven meshes via UV-induced graft polymerization. ASP procedure was followed to mineralize $CaCO_3$ particles on the fiber surface and to form the composite nonwoven meshes. Fourier transform infrared spectroscopy/attenuated total reflectance, field emission scanning electron microscope, equipped X-ray spectroscope, and X-ray diffraction were used to characterize the prepared composite meshes. The mineral cover density increased with the ASP cycles, and it progressively increased for the relative content of calcite in the crystalline part of the mineral layer as well. Contact angle measurements indicate that the as-prepared composite nonwoven meshes were endowed with superhydrophilicity and underwater superoleophobicity, thus they showed prominent application prospects in wastewater treatment and oil/water separation. © 2013 Wiley Periodicals, Inc. J. Appl. Polym. Sci. **2014**, *131*, 39897.

KEYWORDS: composites; electrospinning; surfaces and interfaces; fibers; separation techniques

Received 8 June 2013; accepted 27 August 2013

DOI: 10.1002/app.39897

INTRODUCTION

Polypropylene nonwoven meshes have a broad range of applications in bioseparation,[1] medical protection,[2] membrane bioreactor,[3] and affinity membrane[4] because of their unique characteristics, such as random network of overlapped fibers, overall high porosity, multiple connected pores, high chemical stability, and comparatively low cost.[5,6] However, the inherent hydrophobic nature of polypropylene is an obstacle for their usage as separation media.[7,8] It is widely recognized that the surface properties play a crucial role in separation performance of the nonwoven meshes.[9,10] Therefore, much attention has been paid to enhance the surface hydrophilicity with various methods, such as dip coating, layer-by-layer deposition, chemical treatment, and thermal-/plasma-/UV-/radiation-induced graft polymerization.[11] Among these, UV-induced graft polymerization of hydrophilic polymers, as one of the most effective methods, has attracted widespread and growing interest because of low cost, easy operation, mild reaction condition, and versatility for various vinyl monomers with desirable functionality.[12] Nevertheless, it remains challenging to obtain a uniform spatial distribution of the grafted layer on the fiber surface, which is normally affected by a range of factors, including pretreatment of sample, efficiency of photoinitiator adsorption, and inhomogeneity of UV intensity.[1] Besides, it seems difficult to achieve a superhydrophilic fiber surface even with a high grafting degree by simply tethering hydrophilic polymers such as poly(acrylic acid) (PAA), poly(2-hydroxyethyl methacrylate) (PHEMA), and poly(ethylene glycol) (PEG). Meanwhile, blockage problem is often caused by the headlong pursuit of increasing the amount of grafted PAA, PHEMA, or PEG brushes, which would severely reduce the permeation flux of polypropylene nonwoven meshes.[13,14] Therefore, it is necessary to develop a facile method for the superhydrophilization of the nonwoven meshes.

In recent years, biomineralization has been paid immense attention as it provides a significant self-assembly approach for designing organic/inorganic hybrid composites with hierarchical structures, which show a variety of interrelated mechanical, optical, and magnetic properties.[15,16] In contrast to the rigorous condition in some chemical processes, biomineralization is a mild, low-energy, and pollution-free process, which uses a series of simple and common components in nature. Moreover, one can precisely control the crystal morphology, size, shape, orientation, and aggregation of biominerals from the molecular to

Additional Supporting Information may be found in the online version of this article.

the mesoscopic level by varying regulatory means.[17,18] As one of the most abundant biominerals in the biosphere, calcium carbonate ($CaCO_3$) has been intensively studied because of its diversiform polymorphs and ultrafine structures. Multifarious organic/inorganic hybrids were fabricated by $CaCO_3$-based biomineralization, which can be regulated by both the adsorption of soluble additives on specific faces of the crystals and the template effect of insoluble organic matrices for crystallization. The hybrid materials show a broad range of application prospects in industry and medicine owing to the inexpensiveness and superior biocompatibility of $CaCO_3$.[19,20]

$CaCO_3$ was previously attempted to be introduced on electrospun polymer fibers, such as chitosan, cellulose acetate, and polyamide.[21–23] However, biomineralization methods used were time consuming which required hours to days. The mineral layers were usually developed with uneven coverage of the polymer fibers and sometimes even as a compact film covering the whole surface of the scaffold instead of a single fiber. In addition, there are few literatures concerning the intrinsic hydrophilicity of $CaCO_3$ and its effect on the surface properties of the substrates. This study is the first one to develop a facile and rapid approach for fabricating polypropylene/$CaCO_3$ composite nonwoven meshes and to examine their surface properties and application prospects.

EXPERIMENTAL

Materials

Two kinds of polypropylene nonwoven meshes were used in this work. One (with an average fiber diameter of 13.9 μm $\pm$ 2.3 μm) was prepared by high-temperature electrospinning of isotactic polypropylene/dioctyl phthalate solution in our laboratory,[24] and another (with an average diameter of 6.83 μm $\pm$ 2.6 μm, prepared by melt-blowing) was purchased from Jiang Yin Jinfeng Nonwoven (China). These nonwoven meshes were cut into round pieces (diameter 2.5 cm) and washed with acetone for 0.5 h to remove adsorbed impurities before vacuum drying at 45°C. Acrylic acid (AA, analytical grade) was purchased from Sinopharm Chemical (China) and distilled under reduced pressure before use. Calcium chloride ($CaCl_2$, anhydrous), sodium carbonate (Na_2CO_3, anhydrous), benzophenone (BP), 5-aminofluorescein (AF), 1-ethyl-3-(3-(dimethylamino)propyl)-carbodiimide (EDC), *N*-hydroxysulfosuccinimide (NHS), and other chemicals were all of analytical grade, purchased from Sinopharm Chemical, and used without further purification. Water used in all experiments was deionized and ultrafiltrated to 18.2 MΩ with an ELGA LabWater system (France).

UV-Induced Grafting of PAA on the Nonwoven Meshes

The nonwoven meshes were grafted with PAA by a photoinitiated graft polymerization method.[24] Circular sample was presoaked in 5 mL of 15 m*M* BP/heptane solution for 60 min, dried in air for 30 min, then prewetted with acetone for 5 s, and subsequently immersed into a Petri dish containing 1.5 mL of AA aqueous solution with two sheets of filter paper to clamp the nonwoven mesh. After 5 min of equilibration, irradiation was carried out by UV light (365 nm) for 30 min. The modified nonwoven mesh was washed drastically with water for 24 h to remove excess monomer and homopolymers at ambient temperature. After vacuum drying at 45°C, the grafting degree of PAA (GD_{PAA}) was calculated according to the following equation:

$$GD_{PAA} = \frac{W_1 - W_0}{W_0},$$

where W_1 is the weight of PAA-grafted nonwoven mesh and W_0 is the weight of nascent sample.

Fabrication of Polypropylene/$CaCO_3$ Composite Nonwoven Meshes

$CaCO_3$ formation on the nonwoven meshes was performed by an alternate soaking process (ASP).[25] A 400 m*M* $CaCl_2$ aqueous solution and a 400 m*M* Na_2CO_3 aqueous solution were prepared in advance. The PAA-grafted sample was first prewetted with ethanol for 10 min and washed with water to exchange the ethanol. Then, the sample was immersed in $CaCl_2$ solution and allowed to stand for 30 s, rinsed with water for 30 s, followed by a subsequent immersion in Na_2CO_3 solution for 30 s, and rinsed again with water for 30 s. This procedure was defined as one cycle ASP which needs only 2 min, and the alternate immersion was repeated for a given number of cycles. The nonwoven mesh was rinsed with ethanol to remove any weakly bound $CaCO_3$ following the finish of ASP. After vacuum drying at 45°C, the mineralization degree (MD) of $CaCO_3$ was calculated by the following equation:

$$MD = \frac{W_2 - W_1}{W_1},$$

where W_2 is the weight of polypropylene/$CaCO_3$ composite nonwoven mesh and W_1 is the weight of the PAA-grafted sample.

Instruments and Characterization

Photografting were conducted by a UV light system equipped with a 500-W high-pressure mercury lamp providing homogeneous illumination of up to 100 cm^2 area. Fourier transform infrared spectroscopy (FTIR)/attenuated total reflectance (ATR) spectra were collected on a Nicolet 6700 spectrometer equipped with an ATR accessory (Ge crystal, 45°). Each spectrum was taken by 32 scans at a nominal resolution of 2 cm^{-1}. Surface morphology of the nonwoven meshes was observed by field emission scanning electron microscope (SEM; Hitachi S4800, Japan), and the equipped X-ray spectroscope was used to map the calcium element on the nonwoven mesh surface. To determine the average fiber diameter of the nonwoven meshes, at least 10 fibers were selected from the SEM picture and measured by ImageTool. X-ray diffraction (XRD) was performed using a Rigaku D/Max-2550PC X-ray diffractometer (Japan). Static water contact angle (WCA) and oil contact angle (OCA) were determined by the sessile drop method using a CTS-200 contact angle system (Mighty Technology, China) at room temperature. Briefly, a water drop ($\sim$ 2 μL) was lowered onto the dry surface for WCA, and an oil drop (about 1.5 μL) was dropped carefully onto the nonwoven mesh which was

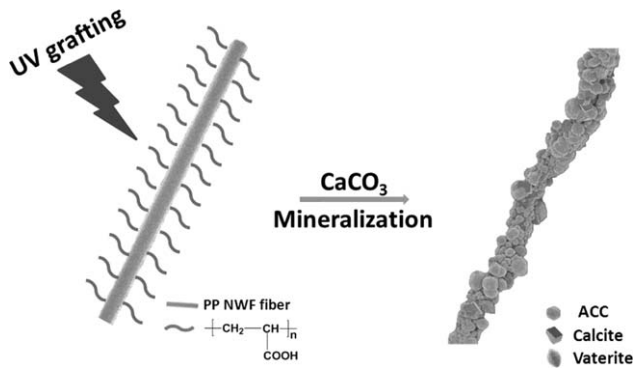

Scheme 1. Schematic illustration for the preparation process of 2polypropylene/calcium carbonate composite fiber.

immersed in water for OCA. The contact angle was recorded after 5 s, and the measurement of each sample was repeated for five times.

The distribution of carboxyl groups on the polypropylene fibers of nonwoven mesh was observed by confocal laser scanning microscope (CLSM). For this purpose, carboxyl groups of the PAA-grafted nonwoven mesh were first activated using EDC/NHS for 2 h, then fluorescently labeled with AF using the condensation reaction between the activated carboxyl groups of PAA and the amino groups of AF in the PBS buffer solution at pH 7.4 for 12 h (molar ratio, —COOH:EDC:NHS:—NH_2 = 1 : 3 : 5 : 20). CLSM was performed with a Leica TCS SP5 confocal setup mounted on a Leica DMI 6000 CS inverted microscope (Leica Microsystems, Wetzlar, Germany) and was operated at an excitation wavelength of 488 nm.

RESULTS AND DISCUSSION

Fabrication of the Polypropylene/$CaCO_3$Composite Nonwoven Meshes

Scheme 1 shows the process of preparing a single polypropylene/$CaCO_3$ composite fiber for the nonwoven meshes. Negatively charged PAA brushes were first tethered on the fiber surface of nonwoven meshes by photoinitiated graft polymerization, and then the grafted nonwoven meshes were alternatively soaked in $CaCl_2$ and Na_2CO_3 aqueous solution to create a mineral covering layer on the fiber surface. It is widely acknowledged that the carboxyl groups of PAA can ionically bind Ca^{2+} ions, resulting in the local supersaturation of Ca^{2+} ions on the fiber surface, which induce the nucleation of $CaCO_3$ on the scaffold instead of in the bulk solution during the mineralization procedure.[21] Therefore, we speculated that the amount and the distribution of grafted PAA on the fiber surface exert an influence on the $CaCO_3$-based mineralization, which further modulate the morphology of $CaCO_3$ particles and cover density of mineral layer on the nonwoven meshes. Here, we investigated the effects of these two factors on the fabrication of polypropylene/$CaCO_3$ composite nonwoven meshes.

It is easy to regulate the amount of grafted PAA on the electrospun nonwoven meshes by changing the monomer concentration during the graft polymerization. The GD_{PAA} increases from 15.1 to 41.7 wt % with the increase of AA concentration from 5 to 15% (v/v) [Figure 1(a)]. Characteristic peaks of the carboxyl group are getting stronger accordingly in FTIR spectra [Figure 1(b)]. The results from five ASP cycles of mineralization reveal that the cover density of mineral layer increases with the GD_{PAA} on the fiber surface of the nonwoven meshes, demonstrating the significance of this factor (Supporting Information Figure S1). On the other hand, even when the grafting degree is more than 40 wt %, the morphology of the electrospun nonwoven meshes is mostly retained except that the fiber surface gets smooth slightly, as can be seen from Figure 2(a,b). Meanwhile, Figure 2(c) shows that the fluorescence intensity is homogenous for the AF-labeled samples. It demonstrates that PAA is uniformly tethered on the surfaces of the whole mesh as well as on each single fiber. This uniformity may be due to the wrinkled morphology of the fiber surface, which can significantly improve the adsorption of photoinitiator to the fiber and then results in relatively homogeneous tethering of PAA chain on the fiber surface in the grafting process.[4] When melt-blown nonwoven meshes were used for comparison, we found that PAA distributes less homogenously on the mesh and fiber surfaces than those

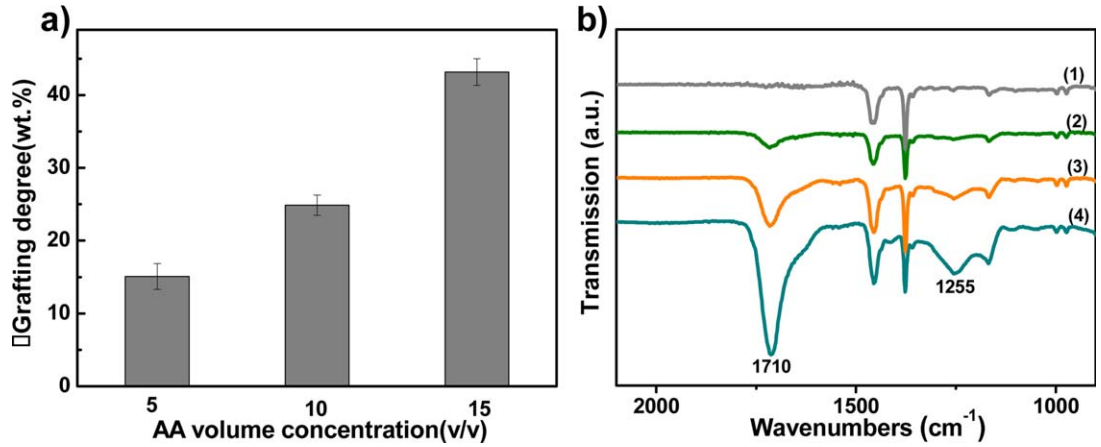

Figure 1. (a) Effects of AA volume concentration on the grafting degree of PAA. (b) ATR/FTIR spectra of the nonwoven meshes with different grafting degrees of PAA: (1) 0, (2)15.1, (3) 26.0, and (4) 41.7 wt %. [Color figure can be viewed in the online issue, which is available at wileyonlinelibrary.com.]

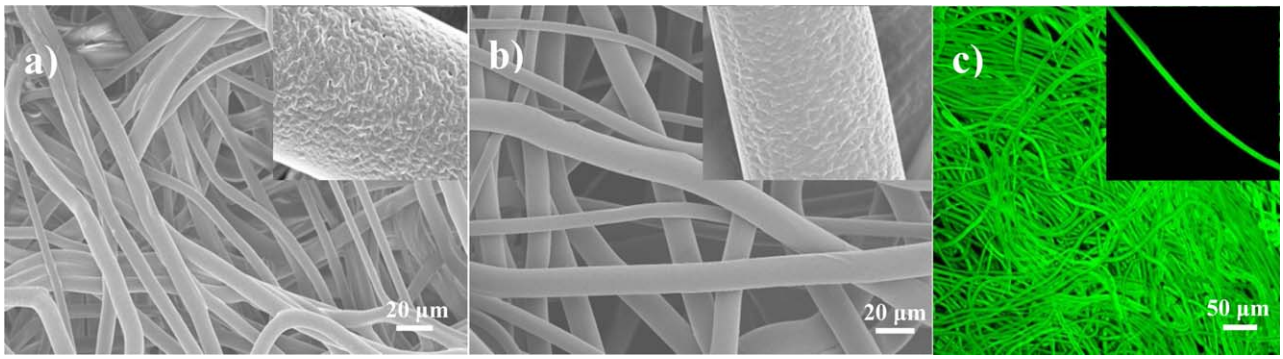

Figure 2. Surface morphology of nascent (a) and grafted (b) electrospun polypropylene nonwoven meshes. The insets are the enlarged view of the fiber surfaces (×10,000). (c) CLSM image of the 5-aminofluorescein-labeled PAA-grafted electrospun nonwoven mesh with a grafting degree of 41.7 wt %. The inset is the view of a single fiber. [Color figure can be viewed in the online issue, which is available at wileyonlinelibrary.com.]

on the electrospun sample (Supporting Information Figures S2 and S3). Correspondingly, the mineral layer evenly covers the whole surface of a single fiber in the electrospun nonwoven meshes, whereas some uncovered spots and big mineral particles appear on the melt-blown ones (Supporting Information Figure S4). These results clearly show the importance of PAA uniformity on the fiber surface for mineralization. On the basis of the above results, we confirm that the GD_{PAA} influences the mineral coverage density on the fiber surface and that a uniform grafting layer results in a homogenous mineralization effect. Hence, in the following experiments, we used the electrospun polypropylene nonwoven mesh with GD_{PAA} of $\sim$ 40 wt % to prepare the polypropylene/$CaCO_3$ composite meshes unless otherwise specified.

The composites were fabricated by alternatively soaking the PAA-grafted nonwoven mesh in $CaCl_2$ solution and Na_2CO_3 solution. This ASP is characterized for its simple and short-time operation, thus it is frequently used for the rapid preparation of organic/inorganic composite materials.[26,27] It can be clearly seen that as ASP proceeds, the polypropylene fiber is gradually covered with mineral particles by its heterogeneous nucleation and growth (Figure 3). The amount and size of $CaCO_3$ particles are

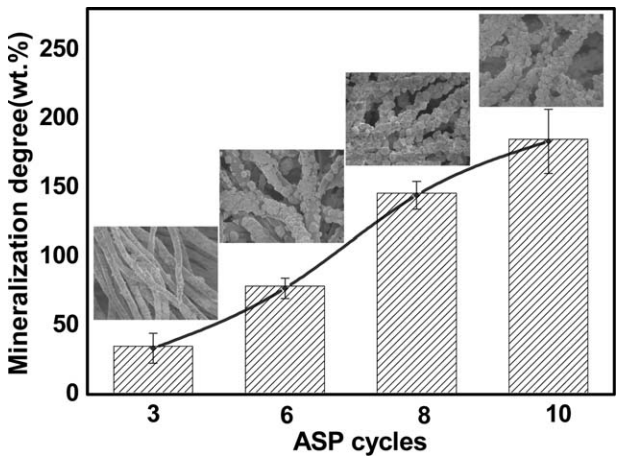

Figure 3. Relationship between the ASP cycles and the mineralization degree of $CaCO_3$ on nonwoven mesh with a grafting degree of $\sim$ 40 wt %. The insets are SEM images of the samples.

influenced by the number of ASP cycles; in general, they rise with the ASP cycles on the nonwoven mesh fibers. For example, the size of mineral particles increases from 1–2 μm to 5–7 μm with the ASP cycle from 3 to 10. In the mineralization process, the initial nucleation of $CaCO_3$ on the fiber surface could be more homogeneous owing to the uniformity of grafted PAA, facilitating the dense coverage of the nonwoven mesh fibers by growing $CaCO_3$ particles. As can be seen from Figure 3 and the element mapping of calcium (Supporting Information Figure S5), the PAA-grafted nonwoven mesh could achieve a desired mineralization effect within 20 minutes (10 ASP cycles), which is considerably faster than the conventional biomimetic process.[21,28]

Structures of the Polypropylene/$CaCO_3$Composite Nonwoven Meshes

ATR/FTIR spectra are shown in Figure 4(a) for the mineralized nonwoven meshes prepared by different ASP cycles. New peaks emerge which can be assigned to the characteristic vibration of $CaCO_3$ at 1410 cm^{-1} (ν_3, carbonate asymmetric stretch) and 874 cm^{-1} (ν_2, out-of-plane bending). These peaks gradually strengthen, manifesting the increase of MD during ASP. Moreover, the characteristic peak of the carbonyl groups shifts from 1710 to 1556 cm^{-1}, indicating the ionization of carboxylic acid groups in PAA brushes.[29] On the other hand, as the size of $CaCO_3$ particles increases, the ATR/FTIR signal of the carbonyl groups could be effectively blocked by the intensive growth of mineral layer on the fiber surface, even causing the absence of peak at 1556 cm^{-1} in the sample of 10 ASP cycles. Simultaneously, a distinguished peak at 712 cm^{-1} (ν_4, calcite, in-plane bending) appears in the spectra, suggesting the formation of calcite in mineralization. Besides, it should be noted that amorphous calcium carbonate (ACC) is readily formed during this quick ASP and that PAA can stabilize ACC to some extent by adsorbing on the high-energy crystal faces to inhibit $CaCO_3$ crystallization.[30] Both of them contribute to the formation of ACC, and the absence of peak at 712 cm^{-1} also indirectly demonstrates the presence of ACC in the mineralized samples with lower ASP cycles. However, FTIR spectra only show preliminary results on the structure of $CaCO_3$. We further used XRD to obtain more detailed information about polymorphs of the mineral layer. Figure 4(b) shows the XRD pattern displays

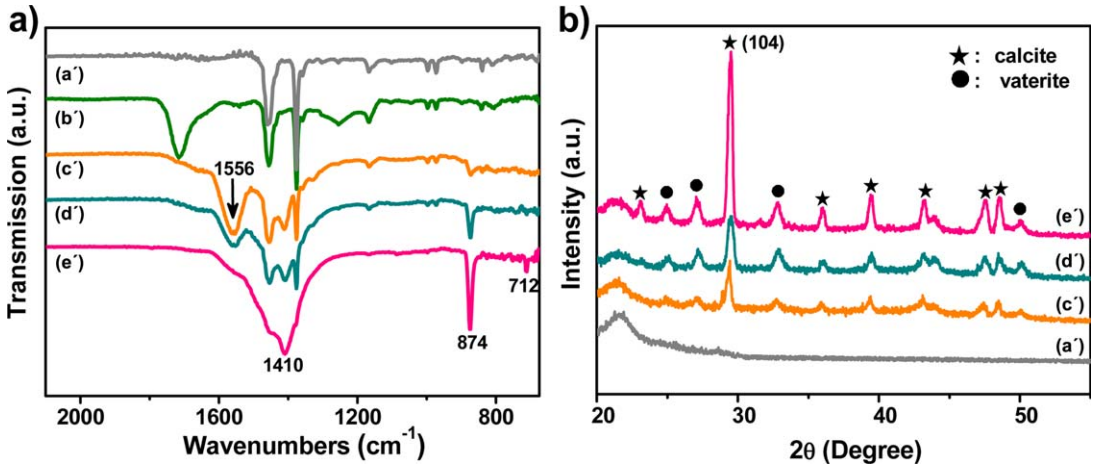

Figure 4. ATR/FTIR spectra (a) and XRD spectra (b) of the studied nonwoven meshes. (a′) Nascent, (b′) PAA-grafted, (c′) mineralized by three ASP cycles, (d′) mineralized by six ASP cycles, and (e′) mineralized by 10 ASP cycles. [Color figure can be viewed in the online issue, which is available at wileyonlinelibrary.com.]

characteristic peaks of calcite at 29.2° (104), 48.3° (116), and 47.3° (018) and of vaterite at 27.0° (112), 32.8° (114), and 50.1° (118), demonstrating that the crystalline part of the mineral layer is actually composed of calcite and vaterite. These are seldom formed in the previous work,[21–23] as a metastable phase in aqueous solution. The rapid mineralization process results in the formation of transitional phase (vaterite) because of its incomplete transformation into the most stable phase (calcite) in short time.[30] In addition, the results from software analysis show that the relative content of calcite progressively increases with the MD (Table I). It can be explained by the Ostwald's Law of Stages.[31] When $CaCO_3$ nucleates and grows in aqueous solution, the unstable phase preferentially forms and continues to break through the energy barrier to form the most stable phase; therefore, calcite which has the most thermodynamically stability accumulates increasingly on the fiber surface. In short, we concluded that the polypropylene/$CaCO_3$ composite nonwoven meshes can be prepared rapidly and that polymorph of the mineral layer is a mixture of ACC, calcite, and vaterite.

Table I. Quantitative Calculation of the Relative Molar Content of Calcite and Vaterite in the Mineralized Samples Prepared by Different ASP Cycles from the Electrospun Polypropylene Nonwoven Mesh Grafted with About 40.0 wt % PAA

Polymorph	3 cycles	6 cycles	10 cycles
Vaterite (%)	71.6	49.3	23.4
Calcite (%)	28.4	50.7	76.6

The calculation was based on the standard reference intensity ratio (RIR) method and reference data from standard XRD cards. RIR of calcite is 2.0 and of vaterite is 1.0.[26]

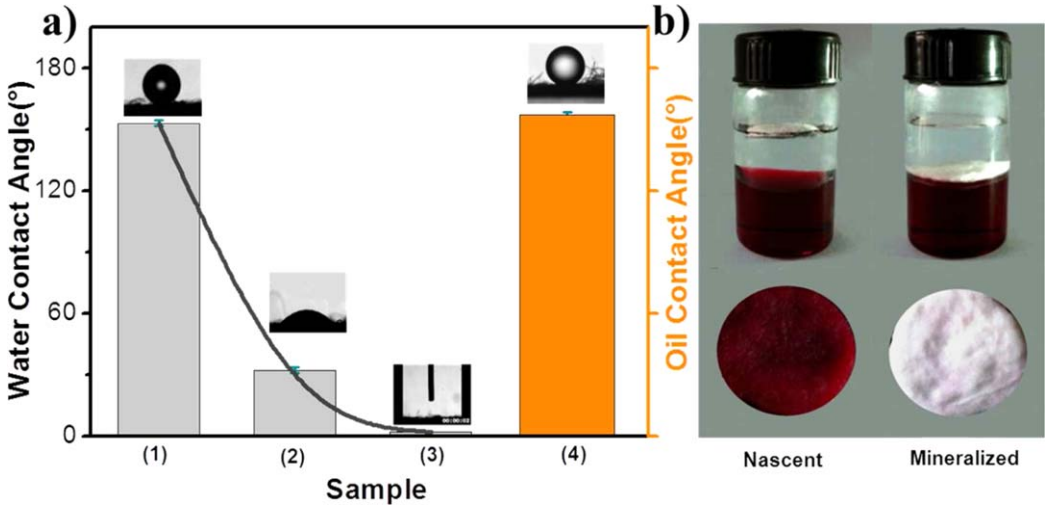

Figure 5. (a) Static water and oil contact angles of the studied nonwoven meshes. (1) Nascent, (2) PAA grafted with a grafting degree of 40 wt %, and (3) and (4) mineralized with a PAA grafting degree of 40 wt % and a mineralization degree of 180 wt %. (b) The nascent and mineralized nonwoven meshes after dipped into staining dichloroethane–water mixture for 5 min with gentle shaking. [Color figure can be viewed in the online issue, which is available at wileyonlinelibrary.com.]

Surface Property and Potential Application of the Polypropylene/$CaCO_3$ Composite Nonwoven Meshes

We first measured the static WCAs to evaluate the wetting properties of the nascent, PAA-grafted, and $CaCO_3$ mineralized nonwoven meshes [Figure 5(a)]. The surface wettability of these nonwoven meshes experience a transition from superhydrophobic ($\theta = 153° \pm 1.7°$), hydrophilic ($\theta = 30° \pm 2.1°$), and to superhydrophilic (θ undetectable). It is believed that such a transition results from the intrinsical hydrophilicity of $CaCO_3$, which can be readily form water hydration layer owing to its high surface free energy and strong polarity. Moreover, it also counts to some extent by the increased surface roughness through the introduction of mineral layer.[32] The as-prepared superhydrophilic composite nonwoven meshes are considered suitable for the application in membrane bioreactor process for wastewater treatment, in which membrane fouling is a serious problem owing to the hydrophobic interactions between bacteria, proteins, and the nonwoven mesh surface.[33]

In addition, the preparation of superoleophobic surface is more difficult than the superhydrophobic surface.[34,35] These superoleophobic surfaces are attracting increasing attention for their great potential as an energy-efficient solution in oil/water separation.[36] We investigated the prospect of the polypropylene/$CaCO_3$ composite nonwoven meshes in the field of oil/water separation. For this purpose, the wetting behaviors of the nascent and mineralized nonwoven meshes in oil/water mixture were examined, which was composed of red oil O staining model oil (1,2-dichloroethane, $\rho = 1.26$ g/mL) and deionized water ($\rho = 1.00$ g/mL). It can be seen from Figure 5(b) that the mineralized one stays at the oil/water interface, whereas the nascent one floats on the water surface because of their different surface properties. It should be noted that the density of the mineralized one is estimated as 1.44 g/cm^3 (Supporting Information), which is larger than the oil density, indirectly indicating that the surface tension instead of the buoyancy force plays a chief role on its wetting behavior in the oil/water mixture. Besides, the nascent nonwoven mesh displays a better oil absorption performance, whereas the mineralized one shows a better oil resistance when they were submerged into the stained 1,2-dichloroethane and taken out after 5 min. We further measured the OCA of the mineralized sample which was immersed in water at ambient temperature. The result reveals that the mineralized nonwoven mesh surface exhibits robust underwater superoleophobicity with a contact angle of $157° \pm 2.4°$. The transition of surface wettability emerges from superhydrophobicity of the nascent nonwoven mesh to superhydrophilicity and underwater superoleophobicity of the mineralized nonwoven mesh. This feature may bring the polypropylene/$CaCO_3$ composite nonwoven meshes potential application in the oil/water separation. Considering the surface properties and high porosity of the bulk material, the composite nonwoven meshes are expected to achieve a gravity-driven and high-throughput separation of oil/water mixture in atmospheric pressure.

CONCLUSION

In summary, we have developed a facile and rapid approach to fabricate polypropylene/$CaCO_3$ composite nonwoven meshes, which is accomplished by UV-induced PAA grafting and then ASP mineralization. The uniform PAA grafting layer enables dense mineral coverage on every single fiber, and a desired mineralization effect can be achieved within 20 min. Meanwhile, the polymorph of the mineral layer is a mixture of ACC, calcite, and vaterite. More interestingly, the surface properties reverse from superhydrophobicity to superhydrophilicity and underwater superoleophobicity after mineralization, thus making these composite nonwoven meshes promising in wastewater treatment and high-throughput oil/water mixture separation.

ACKNOWLEDGMENTS

This work was financially supported by the National Natural Science Foundation of China (Grant no. 50933006). The authors thank Dr. Xiao-Jun Huang and Dr. Ling-Shu Wan for their helpful discussion during the early stages of this work.

REFERENCES

1. Zheng, Y.; Liu, H. Y.; Gurgel, P. V.; Carbonell, R. G. *J. Membr. Sci.* **2010**, *364*, 362.
2. Lin, F. H.; Chen, T. M.; Chen, K. S.; Wu, T. H. *Mater. Chem. Phys.* **2000**, *64*, 189.
3. Chang, W. K.; Hu, A. Y.; Horng, R. Y.; Tzou, W. Y. *Desalination* **2007**, *202*, 122.
4. Wang, C. C.; Yang, F.; Zhang, H. *Sep. Purif. Technol.* **2010**, *75*, 358.
5. Shirazi, M. M.; Bastani, D.; Kargari, A.; Tabatabaei, M. *Desalin. Water. Treat.*, to appear.
6. Shirazi, M. M.; Kargari, A.; Shirazi, M. *J. Desalin. Water. Treat.* **2012**, *49*, 368.
7. Chang, M. C.; Horng, R. Y.; Shao, H.; Hu, Y. *J. Desalination* **2006**, *191*, 8.
8. Zeng, X. F.; Ruckenstein, E. *Ind. Eng. Chem. Res.* **1996**, *35*, 4169.
9. Shirazi, M. J.; Bazgir, S.; Shirazi, M. M.; Ramakrishna, S. *Desalin. Water. Treat.*, to appear.
10. Zhang, C. H.; Yang, F. L.; Wang, W. J.; Chen, B. *Sep. Purif. Technol.* **2008**, *61*, 276.
11. Ye, X. Y.; Xu, Z. K. Polypropylene: Synthesis, Applications and Environmental Concerns; Nova Press: New York, USA, **2012**.
12. Deng, J. P.; Wang, L. F.; Liu, L. Y.; Yang, W. T. *Prog. Polym. Sci.* **2009**, *34*, 156.
13. Yu, H. Y.; Xu, Z. K.; Yang, Q.; Hu, M. X.; Wang, S. Y. *J. Membr. Sci.* **2006**, *281*, 658.
14. Hu, M. X.; Yang, Q.; Xu, Z. K. *J. Membr. Sci.* **2006**, *285*, 196.
15. Kato, T.; Sugawara, A.; Hosoda, N. *Adv. Mater.* **2002**, *14*, 869.
16. Estroff, L. A. *Chem. Rev.* **2008**, *108*, 4329.
17. Mann, S. *Angew. Chem. Int. Ed. Engl.* **2000**, *39*, 3392.
18. Colfen, H.; Mann, S. *Angew. Chem. Int. Ed. Engl.* **2003**, *42*, 2350.

19. Popescu, D. C.; van Leeuwen, E. N. M.; Rossi, N. A. A.; Holder, S. J.; Jansen, J. A.; Sommerdijk, N. *Angew. Chem. Int. Ed. Engl.* **2006**, *45*, 1762.
20. Lee, J. S.; Suarez-Gonzalez, D.; Murphy, W. L. *Adv. Mater.* **2011**, *23*, 4279.
21. Yang, D. Z.; Yu, K.; Ai, Y. F.; Nie, J.; Kennedy, J. F. *Carbohydr. Polym.* **2011**, *84*, 990.
22. Liu, L.; He, D.; Wang, G. S.; Yu, S. H. *Langmuir* **2011**, *27*, 7199.
23. Lakshminarayanan, R.; Valiyaveettil, S.; Loy, G. L. *Cryst. Growth. Des.* **2003**, *3*, 953.
24. Ye, X. Y.; Lin, F. W.; Huang, X. J.; Xu, Z. K. *RSC Adv.* **2013**, *3*, 13851.
25. Taguchi, T.; Kishida, A.; Akashi, M. *Chem. Lett.* **1998**, 711.
26. Ogomi, D.; Serizawa, T.; Akashi, M. *J. Biomed. Mater. Res. A* **2003**, *67*, 1360.
27. Strange, D. G.; Oyen, M. *Acta Biomater.* **2011**, *7*, 3586.
28. Grassmann, O.; Muller, G.; Lobmann, P. *Chem. Mater.* **2002**, *14*, 4530.
29. Kurihara, K.; Kunitake, T.; Higashi, N.; Niwa, M. *Langmuir* **1992**, *8*, 2087.
30. Chen, P. C.; Wan, L. S.; Xu, Z. K. *J. Mater. Chem.* **2012**, *22*, 22727.
31. Threlfall, T. *Org. Process. Res. Dev.* **2003**, *7*, 1017.
32. Sun, T.; Wang, G.; Feng, L.; Jiang, L. *Angew. Chem. Int. Ed. Engl.* **2004**, *43*, 357.
33. Liu, L.; Xu, Z. H.; Song, C. Y.; Gu, Q. B.; Li, F. S. *Desalination* **2006**, *201*, 198.
34. Tuteja, A.; Choi, W.; Ma, M.; et al. *Science 2007*, *318*, 1618.
35. Zhao, H.; Law, K. Y.; Sambhy, V. *Langmuir* **2011**, *27*, 5927.
36. Kintisch, E. *Science* **2010**, *329*, 735.